SUPPLEMENTARY MATERIAL

The metalloprotease ADAMTS4 generates N-truncated Aβ4-x species and marks oligodendrocytes as a source of amyloidogenic peptides in Alzheimer's disease

Susanne Walter, Thorsten Jumpertz, Melanie Hüttenrauch, Isabella Ogorek, Hermeto Gerber, Steffen E. Storck, Silvia Zampar, Mitko Dimitrov, Sandra Lehmann, Klaudia Lepka, Carsten Berndt, Jens Wiltfang, Christoph Becker-Pauly, Dirk Beher, Claus U. Pietrzik, Patrick Fraering, Oliver Wirths*, and Sascha Weggen*

* Correspondence: Oliver Wirths (owirths@gwdg.de) or Sascha Weggen (sweggen@hhu.de)

The supplementary material comprises figures S1-S9, supplementary tables 1-5, and supporting references

Figure S1

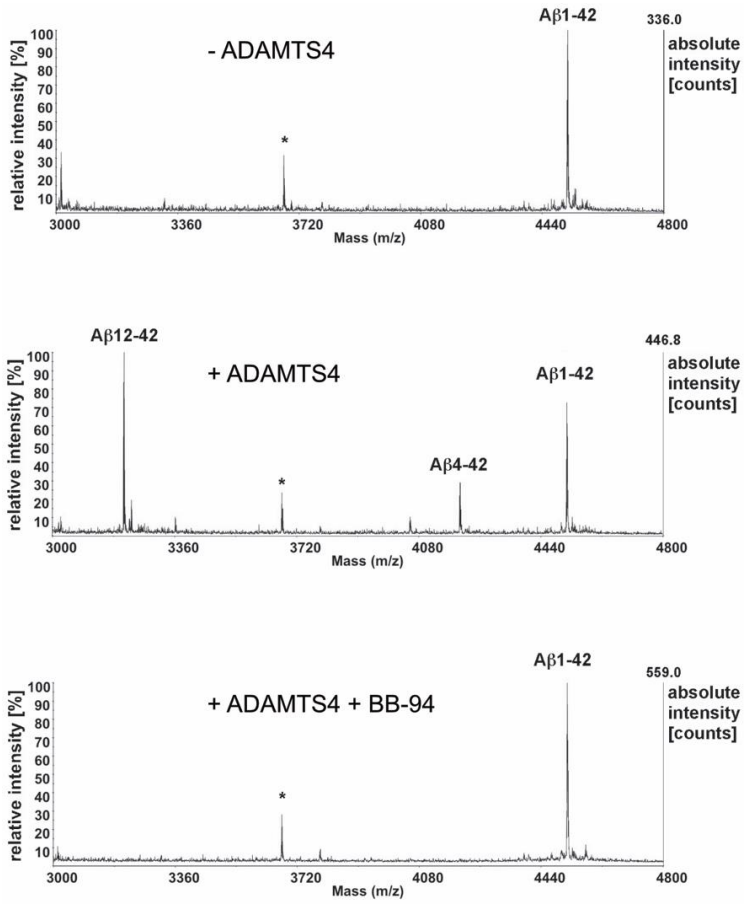

Fig. S1

In vitro digest of synthetic Aβ1-42 peptides with recombinant ADAMTS4. 25 ng of synthetic Aβ1-42 peptides were incubated with 1 μg of a recombinant, catalytically active fragment of human ADAMTS4 encompassing amino acid residues Phe^{213}-Cys^{685} for 24 h at 37 °C, and the resulting Aβ peptide species were analyzed by immunoprecipitation followed by MALDI mass spectrometry. After the co-incubation of enzyme and substrate, peaks corresponding to both Aβ4-42 and Aβ12-42 were observed in the mass spectra (middle panel), indicating that Aβ1-42 peptides could serve as a substrate for ADAMTS4 and that both putative ADAMTS4 cleavage sites in the Aβ sequence starting with the Glu residues 3 and 11 were recognized by the recombinant enzyme. Importantly, these mass peaks were not seen when Aβ1-42 peptides were incubated without the enzyme (upper panel), or when enzyme and substrate were incubated in the presence of 10 μM of the broad-spectrum metalloprotease inhibitor batimastat (BB-94; lower panel). Two independent biological experiments were performed (n=2), and representative mass spectra are shown. The measured monoisotopic masses and the expected masses, and the primary amino acid sequences of the detected Aβ peptides are shown in Supplementary Table 3.

Figure S2

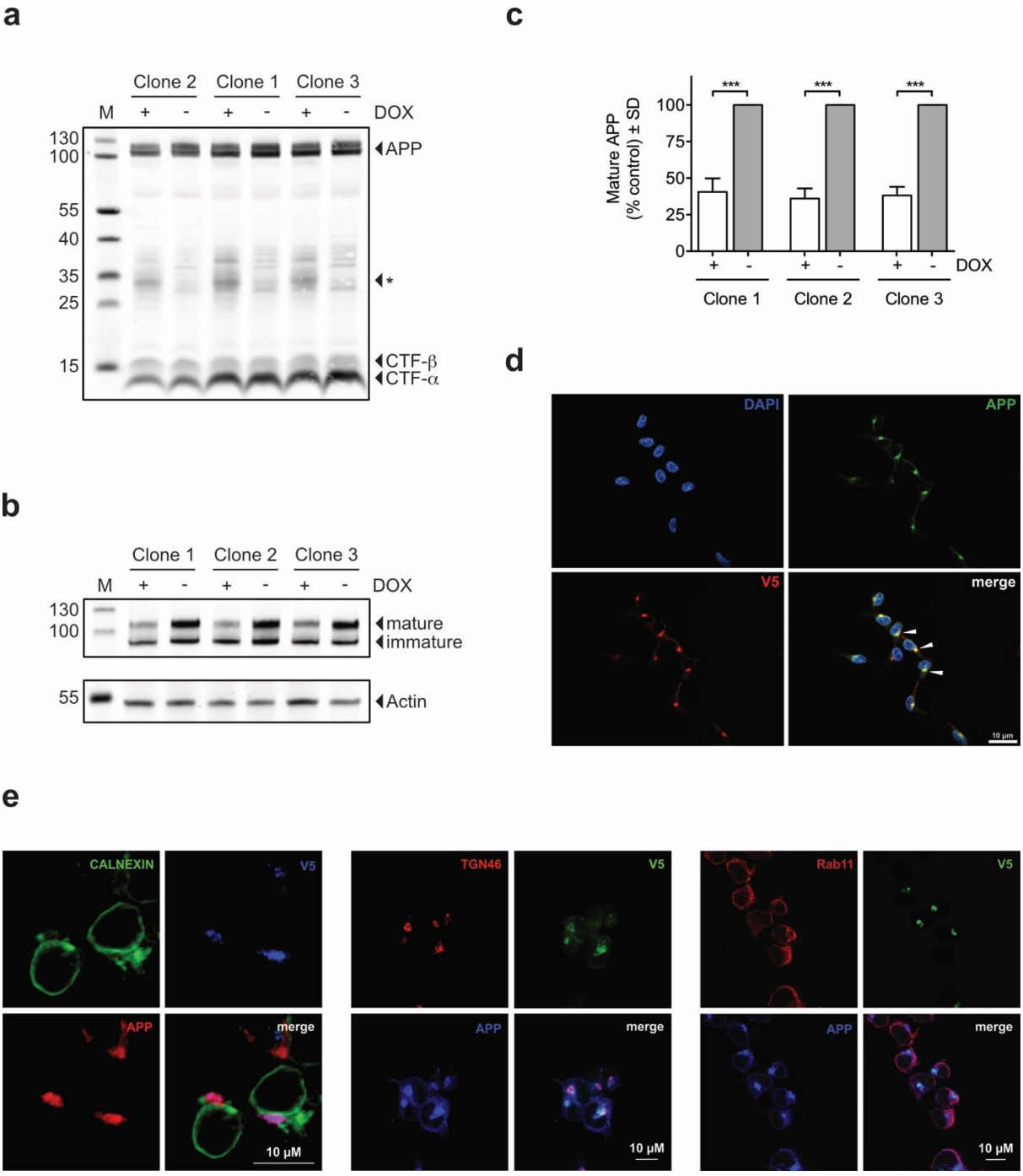

Fig. S2 APP processing in cells with inducible overexpression of ADAMTS4.

a Three single cell clones of HEK-APP695sw/TetOn-ADAMTS4 cells were treated for 48 h with DOX (100 ng/ml) to induce ADAMTS4 expression, and cell lysates were analyzed by Western blotting with polyclonal antibody CT-15 against the C-terminus of APP. When cell lysates were separated on a 12 % SDS-PAGE gel, no substantial differences in full-length APP levels were observed between DOX-induced and non-induced control cells, and levels of the α- and β-secretase generated APP C-terminal fragments (CTF-α and CTF-β)

appeared unchanged. However, an additional C-terminal fragment with a molecular weight between 25-35 kDa was detected in ADAMTS4 expressing cells (marked with *). Three independent biological experiments were performed (n=3), and one representative experiment is shown. **b** Closer inspection of APP levels after separation of cell lysates on 7 % SDS-PAGE gels and Western blotting with antibody CT-15 revealed that ADAMTS4 overexpression reduced the mature, glycosylated forms of APP localized to late compartments of the secretory pathway and the cell surface, while the levels of immature APP remained unchanged. To control for equal protein loading, the same blotting membrane was re-probed with an anti-actin antibody. Three independent biological experiments were performed (n=3), and one representative experiment is shown. **c** Quantification of mature APP levels in HEK-APP695sw/TetOn-ADAMTS4 cells. DOX-induction of ADAMTS4 expression reduced mature APP levels in all three cell clones by more than 50% as compared to non-induced control cells. The signal intensities of the mature APP forms were quantified, normalized to actin levels, and averaged from three independent biological experiments. Subsequently, the mature APP values of non-induced control cells were set to 100%, and the levels of DOX-induced cells were calculated as % control for each cell clone. Unpaired t-test was used to compare the mean relative signal intensities from DOX-induced cells and non-induced control cells. *** $p < 0.001$. **d** Immunocytochemistry for ADAMTS4 and APP in HEK-APP695sw/TetOn-ADAMTS4 cells. ADAMTS4 expression was induced with DOX (100 ng/ml) for 24 h, and V5-tagged ADAMTS4 (red) and APP (green) were stained with anti-V5 and CT-15 antibodies. Co-localization indicated by the yellow overlay color (arrows) was observed close to the DAPI-stained nuclei (blue), presumably in the Golgi compartment. **e** Additional triple immunofluorescence stainings with organelle specific markers revealed co-localization of APP and ADAMTS4 with the Golgi marker TGN46 (middle panel), but not with the endoplasmic reticulum marker calnexin (left panel). The late endosome marker Rab11 showed partial co-localization with APP but not with ADAMTS4 (right panel).

Figure S3

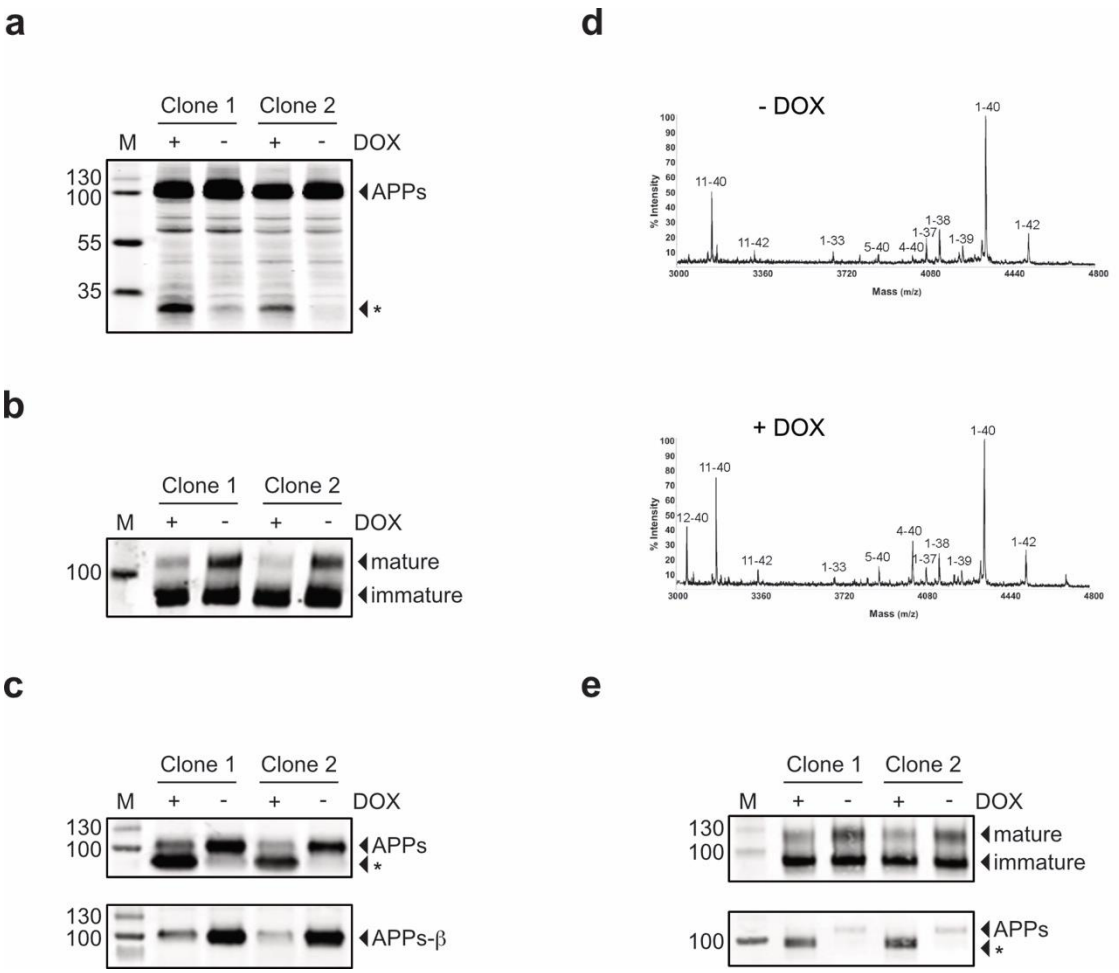

Fig. S3 Processing of overexpressed wild type and endogenous APP in cells with inducible overexpression of ADAMTS4.

a HEK293 cells with stable overexpression of human, wild type APP695 were transduced with a lentiviral vector system that conferred stable, DOX-inducible expression of V5-tagged human ADAMTS4 (HEK-APP695wt/TetOn-ADAMTS4 cells). Single cell clones were induced with DOX (100 ng/ml) for 48 h, and cell lysates were analyzed by Western blotting with antibody CT-15 against the C-terminus of APP. While full-length APP levels appeared similar between DOX-induced and non-induced control cells, ADAMTS4 expressing cells showed a novel APP C-terminal fragment that migrated below the 35 kDa molecular weight marker (marked with *). Much lower levels of this fragment were also observed in non-induced control cells, likely due to leaky expression of ADAMTS4 in the absence of DOX. **b** Separation of cell lysates on 7 % SDS-PAGE gels and Western blotting with antibody CT-15 revealed that ADAMTS4 overexpression reduced the mature, glycosylated forms of APP while the levels of immature APP remained unchanged. **c** Overexpression of ADAMTS4 reduced APPs levels. HEK-APP695wt/TetOn-ADAMTS4 cells were induced with DOX for 24 h. Medium was changed and conditioned for another 24 h in the presence of DOX. Western blotting with antibody 22C11 against the N-terminus of APP (upper panel) revealed a decrease in full-length APPs levels and an additional APPs fragment of approximately 70 kDa (marked with *) in ADAMTS4 expressing cell clones versus non-induced control cells.

Western blotting with anti-APPs-β antibody (lower panel), which recognizes the C-terminal neoepitope generated by β-secretase cleavage of wild type APP, confirmed a substantial reduction in APPs-β levels after induction of ADAMTS4 expression. **d** Mass spectrometry analysis of Aβ peptides in conditioned culture supernatants of HEK-APP695wt/TetOn-ADAMTS4 cells. ADAMTS4 expression was induced with DOX for 48h and supernatants were immunoprecipitated with monoclonal anti-Aβ antibody 4G8 and analyzed by MALDI-TOF mass spectrometry. Spectra of non-induced control cells (-DOX) showed peaks for the common Aβ species such as Aβ1-40, Aβ1-42, and Aβ1-38, and for N-truncated peptides generated by alternative β-secretase cleavage of APP between Tyr10 and Glu11 of the Aβ domain (Aβ11-x). After induction of ADAMTS4 expression (+DOX), additional peaks for Aβ4-40 and Aβ12-40 peptides were clearly detected while other Aβ species remained unchanged. The measured monoisotopic masses and the expected masses, and the primary amino acid sequences of the detected peptides are shown in Supplementary Table 4. **e** HEK-TetOn-ADAMTS4 cells with endogenous APP expression were treated for 48 h with DOX (100 ng/ml) to induce ADAMTS4 expression, and cell-bound and soluble APP metabolites were analyzed. Western blotting of cell lysates (upper panel) with antibody CT-15 against the C-terminus of APP showed reduced levels of the mature, glycosylated forms of APP in DOX-induced versus non-induced control cells, while the levels of immature APP remained unchanged. Western blotting of cell culture supernatants (lower panel) with antibody 22C11 against the N-terminus of APP revealed a decrease in full-length APPs levels and an additional APPs fragment migrating below 100 kDa (marked with *) in ADAMTS4 expressing cell clones versus non-induced control cells. HEK-TetOn-ADAMTS4 cells with endogenous APP expression secreted only minor amounts of Aβ peptides, which did not permit analysis by mass spectrometry or ELISA.

Figure S4

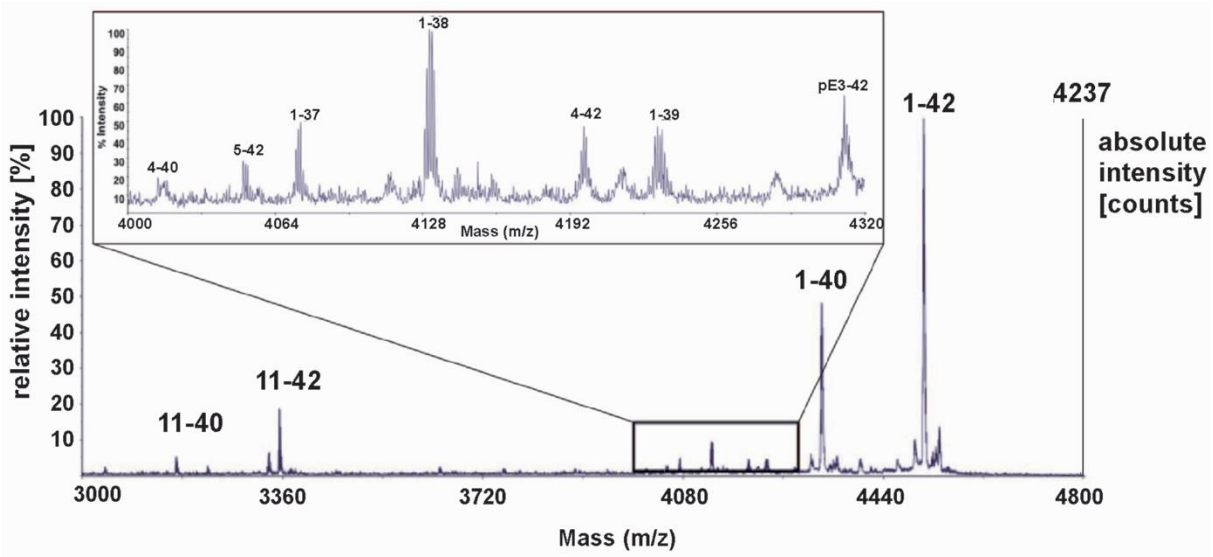

Fig. S4 Mass spectrometry analysis of Aβ peptide species in the 5xFAD model of AD.

Brains of 12-month-old 5xFAD mice were extracted with formic acid, immunoprecipitated with monoclonal antibody 4G8 (against amino acids 17-24 in the Aβ peptide sequence), and analyzed by MALDI-TOF mass spectrometry. In the full spectra, the largest peaks represented Aβ1-42 and Aβ1-40. In enlargements of the spectra (black box), peaks for both Aβ4-40 and Aβ4-42 peptides were clearly visible alongside C-terminally truncated peptides such as Aβ1-37 and Aβ1-38 and other N-terminally truncated peptides such as Aβ5-42 and pyroglutamated AβpE3-42. These mass spectra including the sizes of the Aβ4-40 and Aβ4-42 peaks in relation to the major Aβ1-42 and Aβ1-40 peaks were consistent with previously published mass spectrometry data for the 5xFAD model [2, 3]. Three 5xFAD mice were analyzed (n=3), and a representative mass spectrum is shown. The measured monoisotopic masses and the expected masses, and the primary amino acid sequences of the detected human (Aβ) and murine (mAβ) peptides are shown in Supplementary Table 5.

Figure S5

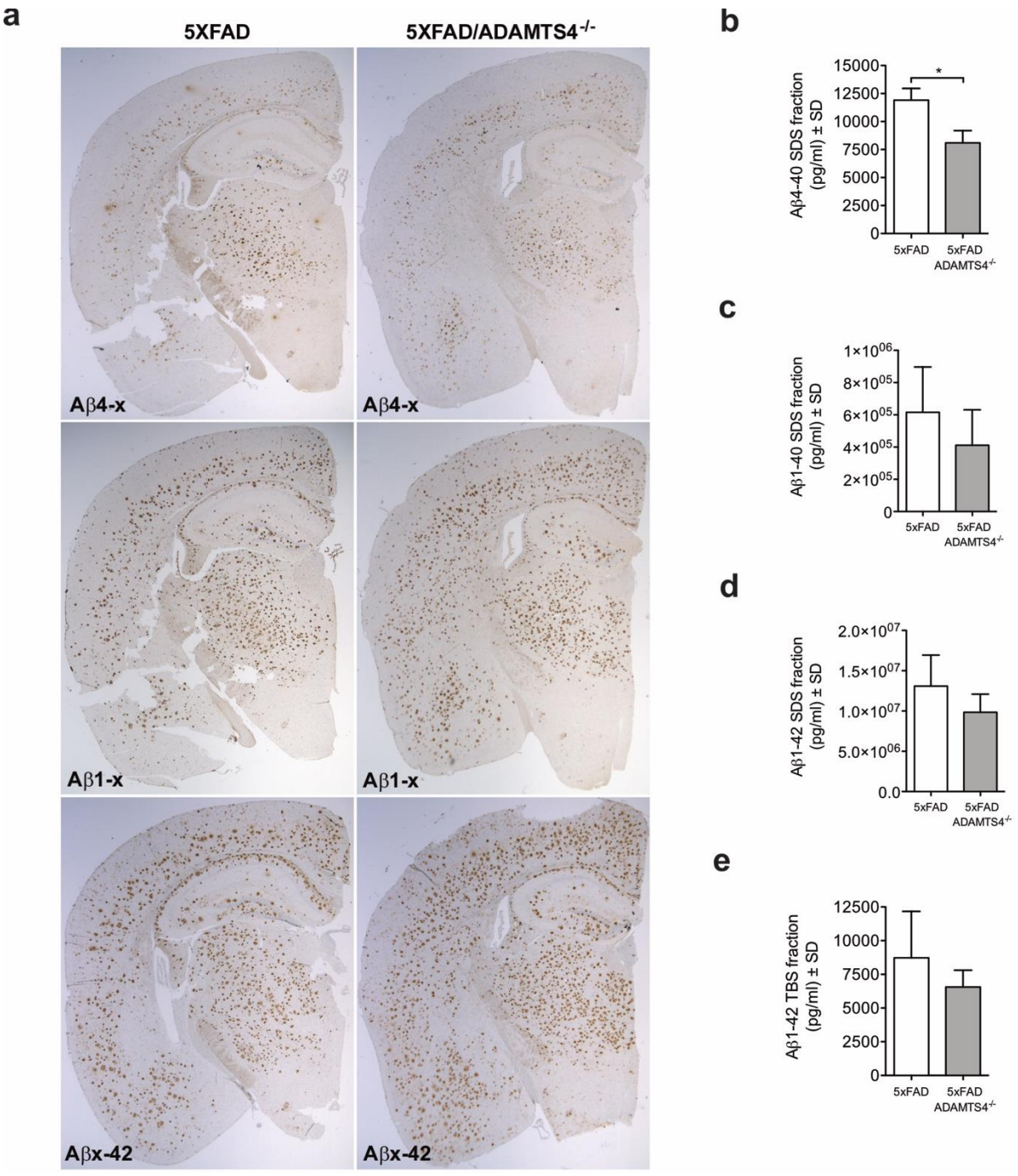

Fig. S5

a Representative coronal brain sections of 12-month-old 5xFAD / ADAMTS4$^{-/-}$ mice and 5xFAD / ADAMTS4$^{+/+}$ control animals. Immunohistochemical stainings were performed with antibody 029-2 against Aβ4-x, antibody 80C2 against Aβ1-x, or antibody D3E10 against Aβx-42 peptides. **b-e** Aβ4-40 and Aβ1-x peptide levels in the TBS and SDS brain fractions of 15-month-old 5xFAD / ADAMTS4$^{-/-}$ mice (n=3) and 5xFAD / ADAMTS4$^{+/+}$ control animals (n=3)**.** Unpaired t-test was used to compare the means between the genotypes. * $p < 0.05$. Aβ4-40 levels were significantly reduced in 5xFAD / ADAMTS4$^{-/-}$ versus 5xFAD / ADAMTS4$^{+/+}$ mice

(**b**), while Aβ1-40 and Aβ1-42 levels in the SDS fractions and Aβ1-42 levels in the TBS fractions were not different between the genotypes (**c-e**).

Figure S6

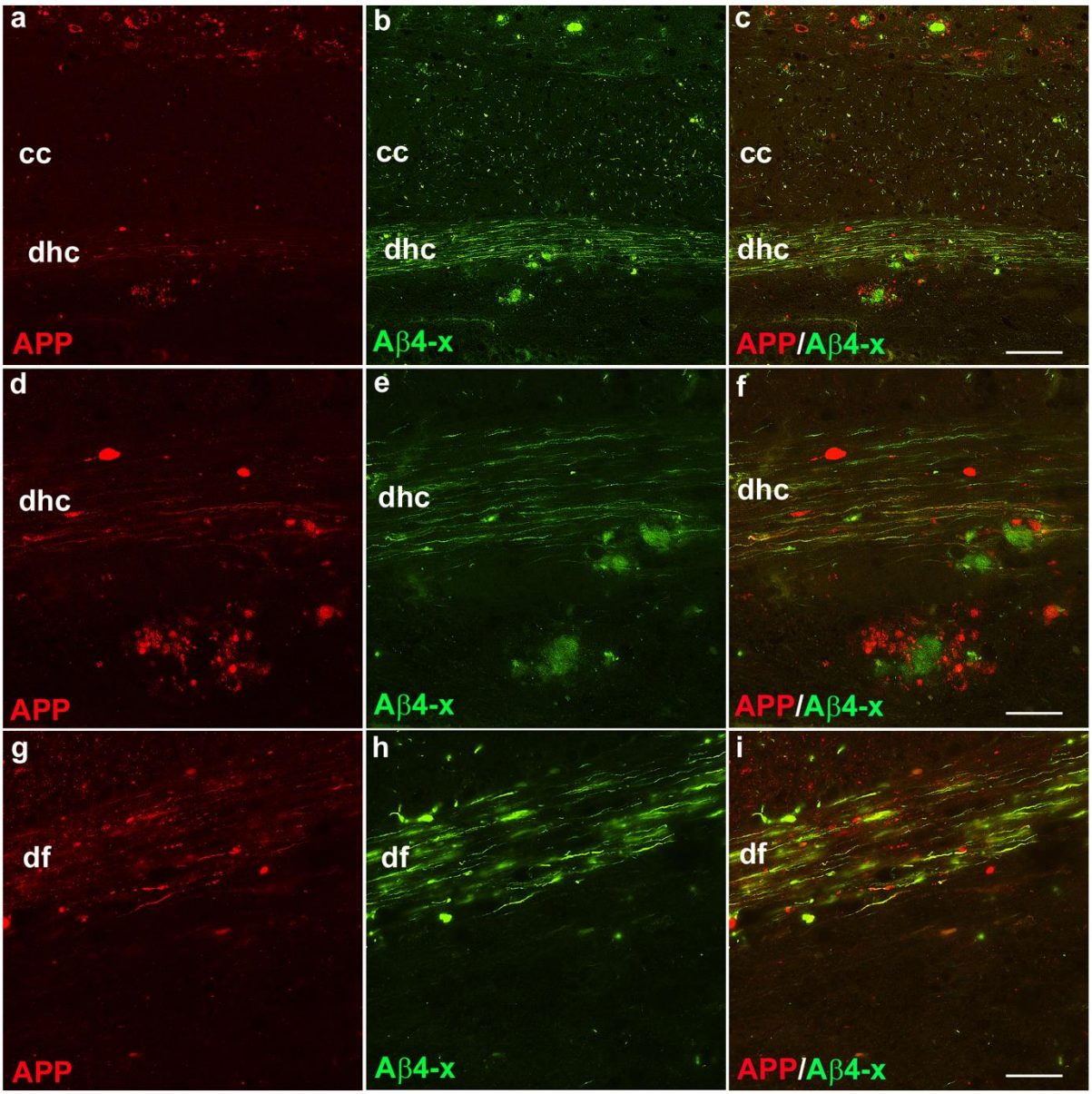

Fig. S6

Double-immunofluorescence staining for APP (**a**, **d**, **g**, red) and Aβ4-x peptides (**b**, **e**, **h**, green) in 12-month-old 5XFAD mice, showing co-localization in the dorsal hippocampal commissure (dhc) underneath the corpus callosum (cc) (**c**, **f**), and in the dorsal fornix (df) (**i**). High-power magnifications of **a-c** are shown in **d-f**. Polyclonal anti-APP antibody was from Synaptic Systems (Cat. No. 127003). Scale bars: (**a-c**): 100 µm; (**d-i**): 33 µm

Figure S7

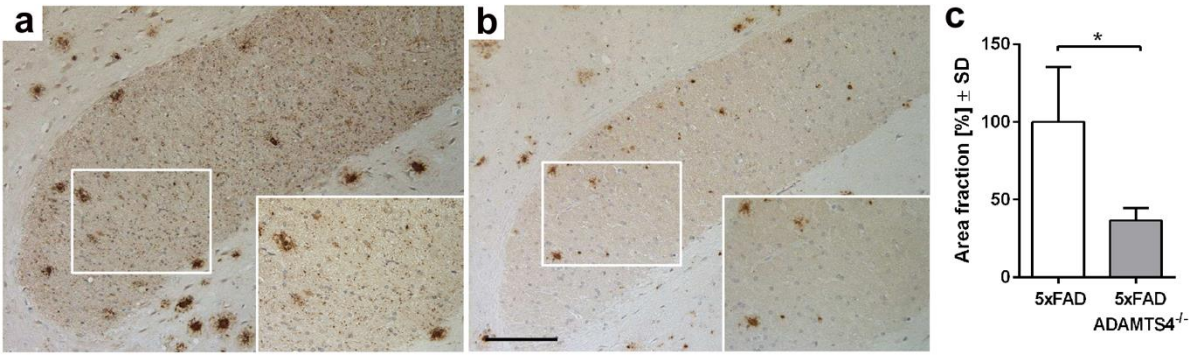

Fig. S7

a Immunohistochemical staining for Aβ4-x peptides with antibody 029-2 showed dot-like immunoreactivity in the corpus callosum of 12-month-old 5XFAD mice. **b** This immunoreactivity was absent in age-matched 5XFAD / ADAMTS4$^{-/-}$ mice. The insets show high-power magnifications of the boxed areas in **a** and **b**. Scale bar: 100 µm. **c** Quantification of 029-2 immunoreactivity in amyloid plaque-free areas of the corpus callosum (n = 4 animals per genotype). Unpaired t-test was used to compare the means between the genotypes. * $p < 0.05$.

Figure S8

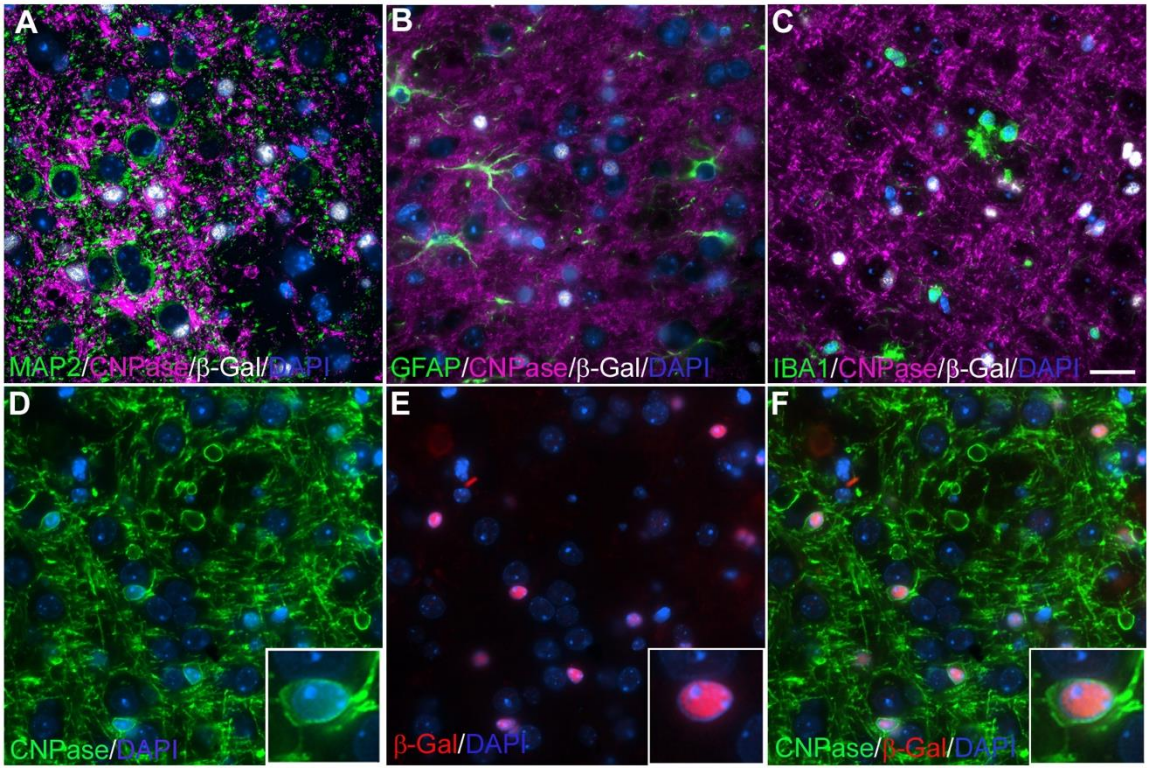

Fig. S8 ADAMTS4 is exclusively expressed in the oligodendrocytic cell lineage in the adult murine brain. The ADAMTS4$^{-/-}$ KO mice were designed as lacZ reporter mice. The ADAMTS4 gene locus was disrupted by insertion of a bacterial lacZ gene such that the endogenous ADAMTS4 gene promotor would drive the expression of β-galactosidase (β-gal). This allowed us to examine the ADAMTS4 expression pattern by β-gal immunohistochemistry. Immunofluorescence co-localization studies were performed on paraffin-embedded cortical brain sections of 6.5-month-old 5xFAD / ADAMTS4$^{-/-}$ mice with antibodies against β-gal and antibodies against marker proteins for neurons and different glial cell types. **a-c** Expression of β-gal (white) did not co-localize with the neuronal marker MAP2 (**a**) (green), the astrocytic marker GFAP (**b**) (green), or the microglia marker Iba1 (**c**) (green). Abundant expression of the oligodendrocyte marker protein 2', 3'-cyclic nucleotide 3'-phosphodiesterase (CNPase, magenta), which is present throughout the oligodendrocytic cell lineage with high expression levels in myelin in the adult CNS [1], was seen. **d-f** In contrast, co-localization of β-gal positive cell nuclei (red) with CNPase (green) was observed. The insets show high-power magnifications of a single oligodendrocyte with β-gal expression in the nucleus and CNPase expression around the nucleus and in cell extensions. Scale bar: 25 µm.

Figure S9

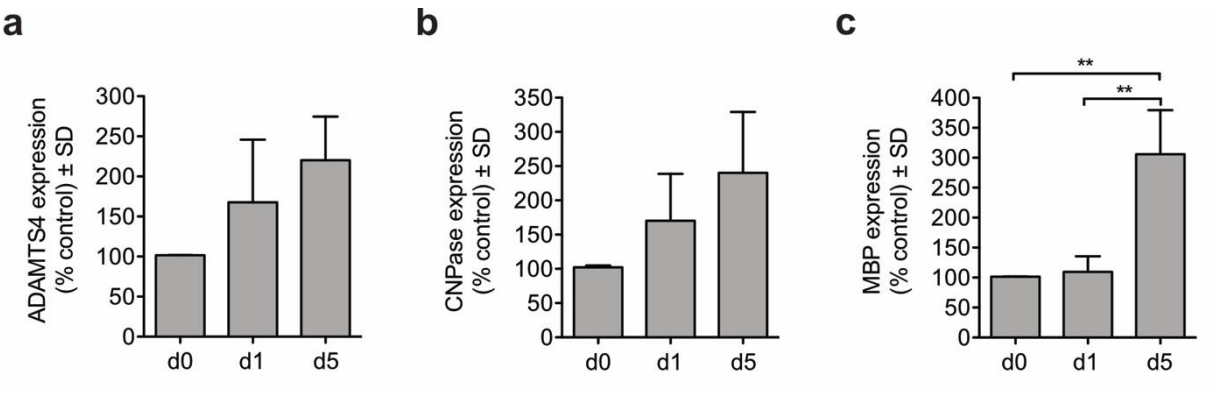

Fig. S9 ADAMTS4 expression in primary murine oligodendrocyte cultures. Oligodendrocyte progenitor cells (OPCs) were extracted from whole brains of newborn C57Bl/6 wild type mice at postnatal days P1-P3 by magnetic cell sorting for the OPC specific cell surface marker A2B5. OPCs were differentiated to mature, myelinating oligodendrocytes by treatment with the thyroid hormones T3 and T4 over a period of 5 days. mRNA was extracted from the cultures before hormone addition (d0), one day after induction of cell differentiation (d1), and at the end of the differentiation process (d5), and analyzed by qPCR. **a** ADAMTS4 mRNA expression was detected both in OPCs at d0 and d1 and in mature oligodendrocytes at d5, with a clear trend for increased expression in the course of the differentiation process. **b** Expression of the oligodendrocyte marker 2', 3'-cyclic nucleotide 3'-phosphodiesterase (CNPase) increased in parallel from d0-d5. **c** Expression of the structural myelin protein myelin basic protein (MBP) was detectable but low in OPCs but increased approximately 3-fold after 5 days in culture, indicating the differentiation of OPCs into myelinating oligodendrocytes. The qPCR analysis was repeated three times. The expression levels of all three genes were normalized to GAPDH expression, and the expression levels at d0 were set to 100%. The mean relative expression levels from all three qPCR measurements were compared by one-way ANOVA with Tukey's post tests. ** $p < 0.01$.

Supplementary Table 1

Measured mass	Expected mass	Δmass (daltons)	Peptide	Position
Spectrum Figure 1d - DOX				
3133.750	3133.440	-0.310	DAEFRHDSGYEVHHQKLVFFAEDVGSN	Aβ1-27
3261.820	3261.535	-0.285	DAEFRHDSGYEVHHQKLVFFAEDVGSNK	Aβ1-28
3673.163	3672.783	-0.380	DAEFRHDSGYEVHHQKLVFFAEDVGSNKGAIIG	Aβ1-33
4013.488	4013.049	-0.439	FRHDSGYEVHHQKLVFFAEDVGSNKGAIIGLMVGGVV	Aβ4-40
4073.438	4072.997	-0.440	DAEFRHDSGYEVHHQKLVFFAEDVGSNKGAIIGLMVG	Aβ1-37
4130.458	4130.019	-0.439	DAEFRHDSGYEVHHQKLVFFAEDVGSNKGAIIGLMVGG	Aβ1-38
4229.592	4229.087	-0.504	DAEFRHDSGYEVHHQKLVFFAEDVGSNKGAIIGLMVGGV	Aβ1-39
4328.571	4328.156	-0.415	DAEFRHDSGYEVHHQKLVFFAEDVGSNKGAIIGLMVGGVV	Aβ1-40
4512.645	4512.277	-0.368	DAEFRHDSGYEVHHQKLVFFAEDVGSNKGAIIGLMVGGVVIA	Aβ1-42
Spectrum Figure 1d + DOX				
3021.996	3021.634	-0.361	VHHQKLVFFAEDVGSNKGAIIGLMVGGVV	Aβ12-40
3674.235	3672.783	-1.452	DAEFRHDSGYEVHHQKLVFFAEDVGSNKGAIIG	Aβ1-33
4013.540	4013.049	-0.491	FRHDSGYEVHHQKLVFFAEDVGSNKGAIIGLMVGGVV	Aβ4-40
4073.552	4072.997	-0.554	DAEFRHDSGYEVHHQKLVFFAEDVGSNKGAIIGLMVG	Aβ1-37
4130.584	4130.019	-0.565	DAEFRHDSGYEVHHQKLVFFAEDVGSNKGAIIGLMVGG	Aβ1-38
4229.540	4229.087	-0.452	DAEFRHDSGYEVHHQKLVFFAEDVGSNKGAIIGLMVGGV	Aβ1-39
4328.843	4328.156	-0.687	DAEFRHDSGYEVHHQKLVFFAEDVGSNKGAIIGLMVGGVV	Aβ1-40
4513.021	4512.277	-0.744	DAEFRHDSGYEVHHQKLVFFAEDVGSNKGAIIGLMVGGVVIA	Aβ1-42

Supplementary Table 2

Measured mass	Expected mass	Δmass (daltons)	Peptide	Position
Spectrum Figure 5c ADAMTS4 +/+				
3151.911	3150.677	-1.234	EVRHQKLVFFAEDVGSNKGAIIGLMVGGVV	Aβ11-40
3262.757	3261.535	-1.222	DAEFRHDSGYEVHHQKLVFFAEDVGSNK	Aβ1-28
3674.024	3672.783	-1.241	DAEFRHDSGYEVHHQKLVFFAEDVGSNKGAIIG	Aβ1-33
4014.343	4013.049	-1.294	FRHDSGYEVHHQKLVFFAEDVGSNKGAIIGLMVGGVV	Aβ4-40
4074.172	4072.997	-1.174	DAEFRHDSGYEVHHQKLVFFAEDVGSNKGAIIGLMVG	Aβ1-37
4130.308	4130.019	-0.289	DAEFRHDSGYEVHHQKLVFFAEDVGSNKGAIIGLMVGG	Aβ1-38
4229.368	4229.087	-1.280	DAEFRHDSGYEVHHQKLVFFAEDVGSNKGAIIGLMVGGV	Aβ1-39
4328.448	4328.156	-0.292	DAEFRHDSGYEVHHQKLVFFAEDVGSNKGAIIGLMVGGVV	Aβ1-40
4513.549	4512.277	-1.272	DAEFRHDSGYEVHHQKLVFFAEDVGSNKGAIIGLMVGGVVIA	Aβ1-42
Spectrum Figure 5c ADAMTS4 -/-				
3151.845	3150.677	-1.168	EVRHQKLVFFAEDVGSNKGAIIGLMVGGVV	Aβ11-40
3262.742	3261.535	-1.207	DAEFRHDSGYEVHHQKLVFFAEDVGSNK	Aβ1-28
3674.043	3672.783	-1.260	DAEFRHDSGYEVHHQKLVFFAEDVGSNKGAIIG	Aβ1-33
4074.162	4072.997	-1.165	DAEFRHDSGYEVHHQKLVFFAEDVGSNKGAIIGLMVG	Aβ1-37
4130.325	4130.019	-0.306	DAEFRHDSGYEVHHQKLVFFAEDVGSNKGAIIGLMVGG	Aβ1-38
4229.469	4229.087	-0.382	DAEFRHDSGYEVHHQKLVFFAEDVGSNKGAIIGLMVGGV	Aβ1-39
4328.554	4328.156	-0.398	DAEFRHDSGYEVHHQKLVFFAEDVGSNKGAIIGLMVGGVV	Aβ1-40
4513.479	4512.277	-1.202	DAEFRHDSGYEVHHQKLVFFAEDVGSNKGAIIGLMVGGVVIA	Aβ1-42

Supplementary Table 3

Measured mass	Expected mass	Δmass (daltons)	Peptide	Position
Spectrum Figure S1 - ADAMTS4				
4512.717	4512.277	-0.440	DAEFRHDSGYEVHHQKLVFFAEDVGSNKGAIIGLMVGGVVIA	Aβ1-42
Spectrum Figure S1 + ADAMTS4				
3205.947	3205.755	-0.191	VHHQKLVFFAEDVGSNKGAIIGLMVGGVVIA	Aβ12-42
4197.547	4197.170	-0.376	FRHDSGYEVHHQKLVFFAEDVGSNKGAIIGLMVGGVVIA	Aβ4-42
4512.738	4512.277	-0.461	DAEFRHDSGYEVHHQKLVFFAEDVGSNKGAIIGLMVGGVVIA	Aβ1-42
Spectrum Figure S1 + ADAMTS4 + BB94				
4512.711	4512.277	-0.434	DAEFRHDSGYEVHHQKLVFFAEDVGSNKGAIIGLMVGGVVIA	Aβ1-42

Supplementary Table 4

Measured mass	Expected mass	Δmass (daltons)	Peptide	Position
Spectrum Figure S3d - DOX				
3150.341	3150.677	0.335	EVHHQKLVFFAEDVGSNKGAIIGLMVGGVV	Aβ11-40
3334.437	3334.798	0.360	EVHHQKLVFFAEDVGSNKGAIIGLMVGGVVIA	Aβ11-42
3673.343	3672.783	-0.560	DAEFRHDSGYEVHHQKLVFFAEDVGSNKGAIIG	Aβ1-33
3865.564	3865.981	0.416	RHDSGYEVHHQKLVFFAEDVGSNKGAIIGLMVGGVV	Aβ5-40
4072.591	4072.997	0.406	DAEFRHDSGYEVHHQKLVFFAEDVGSNKGAIIGLMVG	Aβ1-37
4129.584	4130.019	0.434	DAEFRHDSGYEVHHQKLVFFAEDVGSNKGAIIGLMVGG	Aβ1-38
4228.643	4229.087	0.444	DAEFRHDSGYEVHHQKLVFFAEDVGSNKGAIIGLMVGGV	Aβ1-39
4327.750	4328.156	0.405	DAEFRHDSGYEVHHQKLVFFAEDVGSNKGAIIGLMVGGVV	Aβ1-40
4510.782	4512.277	1.494	DAEFRHDSGYEVHHQKLVFFAEDVGSNKGAIIGLMVGGVVIA	Aβ1-42
Spectrum Figure S3d + DOX				
3021.324	3021.634	0.310	VHHQKLVFFAEDVGSNKGAIIGLMVGGVV	Aβ12-40
3150.362	3150.677	0.314	EVHHQKLVFFAEDVGSNKGAIIGLMVGGVV	Aβ11-40
3334.427	3334.798	0.370	EVHHQKLVFFAEDVGSNKGAIIGLMVGGVVIA	Aβ11-42
3673.404	3672.783	-0.621	DAEFRHDSGYEVHHQKLVFFAEDVGSNKGAIIG	Aβ1-33
3865.621	3865.981	0.359	RHDSGYEVHHQKLVFFAEDVGSNKGAIIGLMVGGVV	Aβ5-40
4012.700	4013.049	0.348	FRHDSGYEVHHQKLVFFAEDVGSNKGAIIGLMVGGVV	Aβ4-40
4072.614	4072.997	0.383	DAEFRHDSGYEVHHQKLVFFAEDVGSNKGAIIGLMVG	Aβ1-37
4129.672	4130.019	0.346	DAEFRHDSGYEVHHQKLVFFAEDVGSNKGAIIGLMVGG	Aβ1-38
4230.745	4229.087	-1.657	DAEFRHDSGYEVHHQKLVFFAEDVGSNKGAIIGLMVGGV	Aβ1-39
4327.816	4328.156	0.339	DAEFRHDSGYEVHHQKLVFFAEDVGSNKGAIIGLMVGGVV	Aβ1-40
4510.796	4512.277	1.480	DAEFRHDSGYEVHHQKLVFFAEDVGSNKGAIIGLMVGGVVIA	Aβ1-42

Supplementary Table 5

Measured mass	Expected mass	Δmass (daltons)	Peptide	Position
Spectrum Figure S4				
3168.890	3169.719	0.828	EVRHQKLVFFAEDVGSNKGAIIGLMVGGVV	mAβ11-40
3352.960	3353.840	0.880	EVRHQKLVFFAEDVGSNKGAIIGLMVGGVVIA	mAβ11-42
4013.060	4013.049	-0.011	FRHDSGYEVHHQKLVFFAEDVGSNKGAIIGLMVGGVV	Aβ4-40
4050.044	4050.102	0.057	RHDSGYEVHHQKLVFFAEDVGSNKGAIIGLMVGGVVIA	Aβ5-42
4072.982	4072.997	0.015	DAEFRHDSGYEVHHQKLVFFAEDVGSNKGAIIGLMVG	Aβ1-37
4128.960	4130.019	1.058	DAEFRHDSGYEVHHQKLVFFAEDVGSNKGAIIGLMVGG	Aβ1-38
4197.109	4197.170	0.061	FRHDSGYEVHHQKLVFFAEDVGSNKGAIIGLMVGGVVIA	Aβ4-42
4229.052	4229.087	0.035	DAEFRHDSGYEVHHQKLVFFAEDVGSNKGAIIGLMVGGV	Aβ1-39
4327.105	4328.156	1.050	DAEFRHDSGYEVHHQKLVFFAEDVGSNKGAIIGLMVGGVV	Aβ1-40
4511.194	4512.277	1.082	DAEFRHDSGYEVHHQKLVFFAEDVGSNKGAIIGLMVGGVVIA	Aβ1-42

SUPPORTING REFERENCES

1. Baumann N, Pham-Dinh D (2001) Biology of oligodendrocyte and myelin in the mammalian central nervous system. Physiol Rev 81: 871-927.
2. Reinert J, Richard BC, Klafki HW, Friedrich B, Bayer TA, Wiltfang J et al (2016) Deposition of C-terminally truncated Abeta species Abeta37 and Abeta39 in Alzheimer's disease and transgenic mouse models. Acta neuropathologica communications 4: 24. doi: 10.1186/s40478-016-0294-7
3. Wittnam JL, Portelius E, Zetterberg H, Gustavsson MK, Schilling S, Koch B et al (2012) Pyroglutamate amyloid beta (Abeta) aggravates behavioral deficits in transgenic amyloid mouse model for Alzheimer disease. J Biol Chem 287: 8154-8162. doi: 10.1074/jbc.M111.308601